IEEE Access
Multidisciplinary | Rapid Review | Open Access Journal

Received March 31, 2021, accepted April 14, 2021, date of publication April 20, 2021, date of current version May 3, 2021.

Digital Object Identifier 10.1109/ACCESS.2021.3074255

Combine Assembly Quality Detection Based on Multi-Entropy Data Fusion and Optimized LSSVM

SIXIA ZHAO, (Member, IEEE), LIYOU XU, (Member, IEEE), JIAMING ZHANG, SHUAI ZHANG, (Member, IEEE), XIAOLIANG CHEN, (Member, IEEE), AND JUN WEI, (Member, IEEE)

Vehicle and Transportation Engineering Institute, Henan University of Science and Technology, Luoyang 471003, China

Corresponding author: Liyou Xu (xlyou@haust.edu.cn)

This work was supported by the National Key Research and Development Program of China under Grant 2017YFD070020402.

ABSTRACT To solve the problems related to the complex structures, multiple parts, and imperceptible assembly quality of combines, this paper compares the performance of the empirical mode decomposition (EMD), ensemble empirical mode decomposition (EEMD), complete ensemble empirical mode decomposition (CEEMD), complete ensemble empirical mode decomposition with adaptive noise (CEEMDAN) and information entropy features in the detection data of combine assembly quality, and proposes a vibration detection method of combine assembly quality detection based on multi-entropy feature fusion and optimized least squares support vector machine. Firstly, the vibration signals of the combine are decomposed by various adaptive algorithms, and intrinsic modal function (IMF) components are obtained. Three entropy features are extracted from the components of the modes. The features are visualized by t-distributed stochastic neighbor embedding (t-SNE), and the performance of these entropy features in the combine assembly quality detection is analyzed. Secondly, a feature extraction method based on information entropy fusion is proposed. The optimized kernel principal component analysis (KPCA) is used to fuse and reduce the dimension of the entropy features, and form the fusion features. Finally, the extracted features are imported into optimization least squares support vector machine (LSSVM) model for training to judge the working state and assembly quality problem type of combine. The results show that the accuracy of using the unfused entropy features is 82.5%, the accuracy of the fused features is 87.9%. After WOA optimization, the accuracy of the final classification reaches 92.1%, which is better than 89.6% by GA and 90.5% by PSO. It shows that the method proposed in this paper can accurately identify combine problems with different conditions and can be applied to combine assembly quality detection.

INDEX TERMS Combine harvesters, assembly quality detection, adaptive decomposition, feature extraction.

I. INTRODUCTION

As important mechanical products in agricultural production, combine harvesters have many parts and complex assembly procedures. Most combine manufacturers in China judge the assembly quality of combine based on artificial experience, and lack of objective, efficient and rapid quality detection methods. To improve the quality of combines and enhance the automation of the agricultural machinery industry, a quick assembly quality inspection of combines must be performed to ensure their long-term, stable, and failure-free operation [1].

The associate editor coordinating the review of this manuscript and approving it for publication was Mehrdad Saif.

Combines are complex agricultural machines that mainly comprise rotating mechanical parts. An accurate mathematical model for analyzing the assembly quality of an entire combine cannot be easily established because the working parts of the machine interact with one another [2]. Chen Chen *et al.* [3] analyzed the relationship between the modal frequency of an entire machine and the modal frequency of its frame by establishing a 7-degree-of-freedom rigid body vibration model for the main frame and detached frame of a combine harvester and then experimentally verified the accuracy of this model. Li Yaoming *et al.* [4] built a calculation model based on classic transmission path theory, identified the location of structural defects based on abnormal excitation forces, and verified the results on a cleaning test

bench. Chen *et al.* [5] identified the main excitation source frequency of the header vibration and the natural frequency of the header by performing time-frequency domain analysis on the multiple vibration signals of the header. Zhang *et al.* [6] used machine vision to detect the position error of large-span hole groups and to improve the installation position accuracy and then verified the superior accuracy and efficiency of this technology compared with traditional measurement methods. While these methods have achieved favorable results, they all focus on a single component and cannot easily address the interactions among multiple components.

With the recent rapid development of fault diagnosis technologies for rotating machinery systems, many fault feature extraction methods have emerged. These methods can be classified into time-domain analysis, frequency-domain analysis, time-frequency analysis, and adaptive signal processing methods. Given the influence of various factors, such as the complex mechanical structures and frictions among components, vibration signals often show non-linear and non-stationary characteristics [7]. Compared with traditional time-frequency domain and wavelet packet analyses, the adaptive decomposition method is more intuitive and adaptive given that no basis function needs to be preset. Accordingly, this method has attracted wide usage used in the field of fault diagnosis [8]–[10]. Empirical mode decomposition (EMD) is a recursive mode decomposition method that uses the extreme points of the original signal to perform multiple envelope calculations. Given that general vibration signals contain noise or intermittent interference signals, the estimation error that arises during envelope calculation is amplified by multiple recursive decompositions, thereby leading to the modal aliasing of the decomposition results [11]. To improve empirical mode decomposition (EMD), ensemble empirical mode decomposition (EEMD), complete ensemble empirical mode decomposition (CEEMD) and complete ensemble empirical mode decomposition with adaptive noise (CEEMDAN) have been proposed, and obtained a lot of applications [12]–[15]. Zhang *et al.* [16] used CEEMD and t-test to reconstruct the time series of rainfall, reservoir water level and other inducing factors into high-frequency components and low-frequency components respectively. The ant colony optimization based support vector machine regression was used to predict TGRA. Niu *et al.* [17] established a hybrid prediction model combining random forest (RF), improved grey ideal value approximation (IGIVA), complementary ensemble empirical mode decomposition (CEEMD), particle swarm optimization based on dynamic inertia factor (DIFPSO) and back propagation neural network (BPNN), and verified the effectiveness of the hybrid model. Yao and Pan [18] proposed a new empirical mode decomposition (EMD) method based on ECG signal morphological structure adaptive noise algorithm. Based on the characteristics of CEEMDAN, this method can eliminate high-frequency interference and low-frequency baseline drift. Cheng *et al.* [19] used EEMD method to identify the intrinsic mode function of noise and signal, and removed the intrinsic mode function with noise as the main component, which was applied to the actual lidar signal and achieved good denoising effect. However, the process characteristics of the original signal cannot be reasonably expressed and reflected in signal decomposition, resulting in low diagnostic accuracy.

Feature extraction is a key step in fault diagnosis and directly affects the accuracy of classification [20]. At present, Using information entropy for feature extraction has been widely used in the field of mechanical fault diagnosis [21], [22]. Fei *et al.* [23] put forward wavelet correlation characteristic scale entropy method, used process power spectrum entropy (PPSE) and support vector machine (SVM) for bearing fault diagnosis, which provided basis for improving fault diagnosis accuracy of rotating machinery such as gas turbine. Because the information entropy of the characteristic signal will change in different frequency bands, the entropy of each order IMF can be calculated as the fault feature to determine whether there is a fault [24]–[27]. At the same time, different information entropy functions represent the characteristics of the signal at a specific location, it is also important to choose the appropriate entropy function. Min *et al.* [28] and Gao *et al.* [29] extracted multiple entropy of each IMF to form a feature set through adaptive decomposition, but did not consider the dimension of the feature set, resulting in the extracted information entropy feature can not fully reflect the signal features. Therefore, it is urgent to propose an effective method to solve the above problems, so as to improve the effect of fault diagnosis.

Based on the assembly quality inspection process of combine, this paper studies the feature extraction based on multi-entropy fusion and the fault diagnosis method of complex rotating machinery based on optimal least squares support vector machine. In order to study the adaptability of the current methods in the field of rotating machinery fault diagnosis and recognition in the detection of combine assembly quality, based on the above mentioned this paper collects the data of combine assembly quality problems through experiments, and decomposes the original data by using EMD, EEMD, CEEMD, CEEMDAN. After feature extraction of each IMF after decomposition by using energy entropy, fuzzy entropy and permutation entropy, multi-entropy fusion feature set is constructed by KPCA. The performance of various entropy features in combine assembly quality inspection were compared. Finally, based on the analysis results, the assembly quality detection model of the optimized least squares support vector machine combine harvester was established.

II. BASIC PRINCIPLES AND METHODS

A. BASIC PRINCIPLES OF CEEMDAN

CEEMDAN is based on EMD and EEMD. EMD method is to decompose the original signal into a series of IMF components from high frequency to low frequency and a residual component [30]. Different IMF represents the single component signal with different physical meaning in the original signal. However, the mode aliasing phenomenon of EMD method is more serious. EEMD method adds white noise to

the original signal for many times and then decomposes it by EMD. The IMF components obtained by EMD decomposition for many times are averaged to get the final IMF component. The principle of CEEMD is similar to EEMD, which is to add two opposite white noise signals to the original signal and then decompose them by EMD. Both EEMD method and CEEMD method can effectively improve the mode aliasing phenomenon of EMD method, but both EEMD and CEEMD need to be integrated for many times to eliminate the influence of adding white noise and reduce the reconstruction error. The increase of the average number of integration will lead to the increase of calculation and affect the efficiency. CEEMDAN method adds white noise adaptively in each stage of EMD decomposition. No matter how many times of integration average is, the reconstruction error of this method is almost zero. Therefore, the CEEMDAN method not only improves the mode aliasing phenomenon of EMD method, but also solves the problem of large amount of calculation of EEMD and CEEMD methods.

The implementation steps of CEEMDAN are as follows:

(1) Construct signal sequence $X^n(t)$. Firstly, a white noise signal sequence $\omega^n(t)$ with standard deviation of ε is added to the original signal $X(t)$ as follows:

$$X^n(t) = X(t) + \varepsilon_0 \omega^n(t), \quad n = 1, 2, \ldots, K \tag{1}$$

(2) EMD is used to decompose the noise signal sequence $X^n(t)$ to obtain the first-order IMF component sequence and calculate the average component of the first-order IMF.

$$\overline{Imf}_1(t) = \frac{1}{K} \sum_{i=1}^{K} IMF_1^i(t) \tag{2}$$

The residual after decomposition as follows:

$$r_1(t) = X(t) - \overline{Imf}_1(t) \tag{3}$$

(3) On the basis of residuals, the residual signal $r_1(t) + \varepsilon_1 EMD_1(\omega^n(n))$ is obtained by adding white noise. Then EMD decomposition is carried out to obtain the second order IMF component sequence. Then the second order IMF mean component and residuals are calculated.

$$\overline{Imf}_2(t) = \frac{1}{K} \sum_{n=1}^{K} EMD_1\left(r_1(t) + \varepsilon_1 EMD_1\left(\omega^n(t)\right)\right) \tag{4}$$

$$r_2(t) = r_1(t) - \overline{\mathrm{Im}\, f_2}(t) \tag{5}$$

(4) Repeat the above decomposition process according to the same rules. Calculate the k-th residual $r_k(t)$ and $k+1$ IMF mean component $\overline{Imf}_{k+1}(t)$, until the residuals $r_k(t)$ satisfactory formula (8) or cannot be EMD decomposed.

$$r_k(t) = r_{k-1}(t) - \overline{\mathrm{Im}\, f_k}(t) \tag{6}$$

$$\overline{Imf}_{k+1}(t) = \frac{1}{K} \sum_{n=1}^{K} EMD_1 \times \left(r_k(t) + \varepsilon_k EMD_k\left(\omega^n(t)\right)\right) \tag{7}$$

$$\sum_{t=0}^{T} \frac{|r_{k-1}(t) - r_k(t)|^2}{r_{k-1}^2(t)} \le SD_k \tag{8}$$

where T represents the length of signal $X(t)$, $r_k(t)$ represents the residuals resulting from the k-th decomposition.

B. FEATURE EXTRACTION

When the vibration signal contains strong interference and noise, the use of a single surface feature extraction method can easily lead to the reduction of diagnosis accuracy [31]. In recent years, Entropy theory has been applied to mechanical equipment fault diagnosis by many scholars in many forms such as Fuzzy Entropy [32], Sample Entropy [33], and Approximate Entropy [34]. The effectiveness of relevant entropy has been verified to a certain extent [35]–[38]. In this paper, a variety of entropy feature extraction algorithms are used. After signal decomposition, energy entropy, permutation entropy and fuzzy entropy features are extracted. By optimizing KPCA, features are fused and dimension reduced to construct feature data set.

C. LSSVM

Support vector machine (SVM) is a relatively mature machine learning theory that has been widely used in mechanical, electrical, and other related fields. This machine learning method is based on statistical VC dimension theory and the structural risk minimization principle. SVM has unique advantages in nonlinear mapping, including its requirement for less training data and its limits over learning, thereby making this method especially suitable for processing small sample data [39]. Least squares support vector machine (LSSVM) improves the inequality constraint of SVM to equality constraint. It makes the calculation cost lower and simplifies the calculation process of support vector machine.

Suppose that the sample training dataset is:

$$T = \{(x_1, y_1), \cdots, (x_n, y_n)\} \in (X \times Y)^n \tag{9}$$

where $x_i \in X = R^n$, $y_i \in Y = \{1, \cdots, M\}$, $i = 1, \cdots, n$.

To solve the linear non-separable classification problem, SVM performs mapping to transform sample x into a high-dimensional space and then classifies the transformed sample in a high-dimensional space, that is, $\Phi : R^n \to H$. By using $K(x_i, x_j)$ to replace the inner product of the high-dimensional feature space, the optimization problem can be transformed into

$$\min_{\omega,b} J(\omega, \xi) = \frac{1}{2}\omega^T \omega + \frac{1}{2} f \sum_{i=1}^{n} \xi_i^2 \tag{10}$$

$$\text{s.t. } y_i\left[\omega^T \varphi(x_i) + b\right] = 1 - \xi_i \tag{11}$$

where ω is the weight coefficient vector; b is the offset; f is the regularization factor; ξ_i is the relaxation variable; J is the objective function; $\varphi(x_i)$ is the kernel function, which maps the sample set from the input space to the high-dimensional feature space.

The Lagrange function is constructed as follows:

$$L(\omega, b, \xi, \alpha) = J(\omega, \xi) - \sum_{i=1}^{n} \alpha_i \left\{ y_i \left[\omega^T \varphi(x_i) + b \right] - 1 + \xi_i \right\} \quad (12)$$

where α_i is a Lagrangian operator and the optimization condition is:

$$\begin{cases} \dfrac{\partial L(\omega, b, \xi_i, \alpha_i)}{\partial \omega} = 0 \Rightarrow \omega = \sum_{i=1}^{l} \alpha_i y_i \varphi(x_i) \\ \dfrac{\partial L(\omega, b, \xi_i, \alpha_i)}{\partial b} = 0 \Rightarrow 0 = \sum_{i=1}^{l} \alpha_i y_i \\ \dfrac{\partial L(\omega, b, \xi_i, \alpha_i)}{\partial \xi_i} = 0 \Rightarrow \alpha_i = f \xi_i \\ \dfrac{\partial L(\omega, b, \xi_i, \alpha_i)}{\partial \alpha_i} = 0 \Rightarrow y_i \left(\omega^{\mathrm{T}} \varphi(x_i) + b \right) - 1 + \xi_i = 0 \end{cases} \quad (13)$$

By eliminating ξ_i and ω, we can get the following results:

$$\begin{bmatrix} 0 & l^T \\ l & K + f^{-1} I \end{bmatrix} \begin{bmatrix} b \\ \alpha \end{bmatrix} = \begin{bmatrix} 0 \\ y \end{bmatrix} \quad (14)$$

where I is the identity matrix and K is the kernel function matrix.

Then the classification decision function of LS-SVM is as follows:

$$f(x) = \operatorname{sgn} \left[\sum_{i=1}^{n} \alpha_i K(x, x_i) + b \right] \quad (15)$$

By introducing different inner product kernel functions K into the above formula, different least squares support vector machines with different kernel can be formed.

To solve the multi-classification problem in this paper, construct the cyclic model of least squares support vector machine as shown in Figure 1. Multi-objective classification is achieved by cyclically decomposing multi-objective data into multiple binary classification problems.

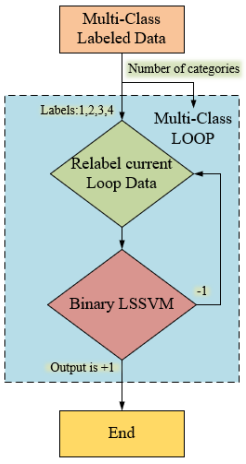

FIGURE 1. Flow chart of the multi-classification LSSVM.

III. ASSEMBLY QUALITY INSPECTION PROCESS

This article uses vibration signals to detect the assembly quality of combined harvesters. Through a decomposition of the vibration signals from the main parts of a combine under random excitation, the energy entropy, permutation entropy and fuzzy entropy of each modal component is obtained as an eigenvector. The optimized LSSVM is then trained and tested after feature dimension reduction and fusion by kernel principal component analysis (KPCA). The implementation process is shown in Figure 3.

The test was performed on September 2019 at the Vehicle Laboratory of the School of Vehicle and Traffic Engineering of the Henan University of Science and Technology. The Zhongshou 4LZ-9A2 rice-wheat combine harvester was used as the combine harvester model in the experiment. The acceleration sensor was used to measure the vibration signal. The sampling frequency was set to 2 kHz. The actual industrial site was simulated and restored under an engine speed of 780 r/min. The data were collected at the measuring points which located at the front bearing seat of the disengaging drum under the cab of the combine as shown in Figure 2.

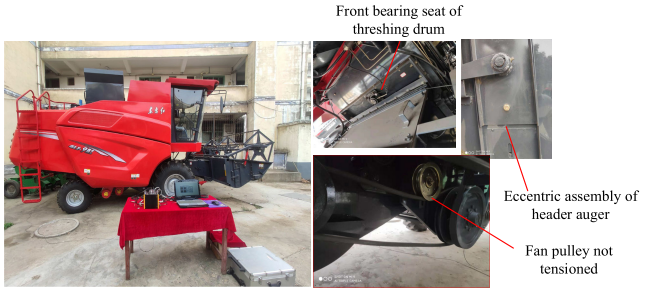

FIGURE 2. Positions of the measuring points on the test harvester.

Three types of problems were injected into the whole machine, namely, the eccentric assembly of the header agitator, two non-tensioned quality defects in the assembly of the fan pulley, and a combination of the two aforementioned problems. The effectiveness of the proposed method was then verified according to the data obtained under four states, namely, the normal state, fault 1, fault 2, and fault 3 states.

The specific steps of the assembly quality inspection process are described as follows:

(1) Obtain the experimental data of the combine under various conditions.

(2) According to the defined sample length, the vibration signals in each state are separately decomposed to obtain several modal components.

(3) Select the first m modal components with the main information to calculate the energy entropy, permutation entropy and fuzzy entropy.

(4) Construct the multi-entropy feature vector and use the KPCA to fusion the entropy features vector. Compare the performance of various entropy using in combine assembly quality detection.

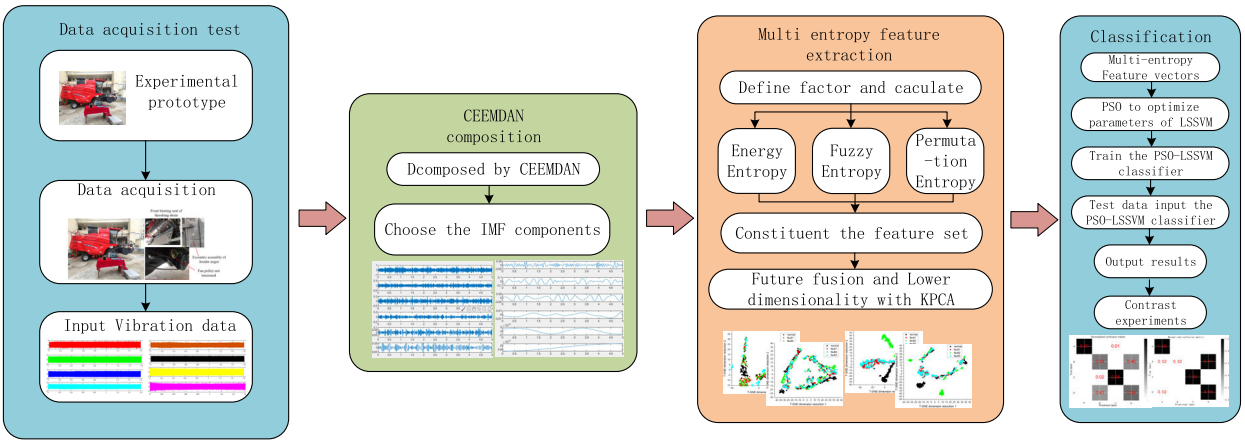

FIGURE 3. Flow chart of the assembly quality inspection.

(5) LSSVM is used as a classifier to classify various assembly quality problems. A variety of optimization algorithms are compared and analyzed.

IV. EXPERIMENT AND ANALYSIS

Taking parts of 4 kinds data signals as an example, the number of signal points was set to 10000 points, and the time-domain waveform and spectrum of the signal are shown in Figure 4. The obvious characteristic frequency of the problem cannot be seen from the figure, thereby highlighting the difficulty of identifying the assembly quality problem of combine harvesters via conventional spectrum analysis.

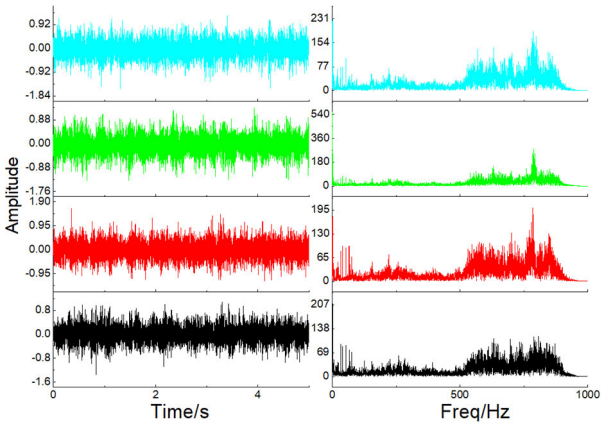

FIGURE 4. Waveform and frequency spectrum of vibration signals from 4 kinds of state.

As shown in Table 1, the data set is constructed from the extracted data of questions 1, 2, 3 and normal vibration. There are 200 groups of four kinds of data, and each group has 10000 data signal points. In each assembly quality problem data set, 70% of them are selected for model training and 30% for testing. In order to verify the effectiveness of the adaptive algorithm, EMD, EEMD, CEEMD, CEEMDAN were used to process the signal, and the decomposed signal was analyzed. Since the fault information is mainly stored in the previous

TABLE 1. Label and order of test set samples.

Test set	Label	Sample matrix sequential labeling
Normal status	A	1～200
Fault 1 status	B	201～400
Fault 2 status	C	401～600
Fault 3 status	D	601～800

IMF components, after decomposing each signal, the energy entropy, fuzzy entropy and permutation entropy of the first 10 IMF are calculated respectively, and the optimized KPCA is used to construct the fusion feature set. t-SNE is used to reduce the dimension visually, and the two-dimensional scatter map of each adaptive algorithm after fusion of multiple entropy features is drawn. LSSVM is used for training and testing. The LSSVM use RBF kernel function, set default parameters gamma = 2 and sigma = 2.

A. ANALYSIS OF SIGNAL DECOMPOSITION RESULTS

Fig. 5, 6 shows the reduced dimension visualization of t-SNE with multiple entropy features after EMD EEMD decomposition and the confusion matrix diagram of classification results with unoptimized LSSVM. Where sub-graph a is the result before normalization of all data, b is the result after normalization. From the t-SNE diagram, it can be seen that the clustering effect of EMD and EEMD data is improved after normalization, especially in normal state and Fault 2, but the overall effect is not obvious, Fault 1 and Fault 3 are obviously difficult to distinguish. According to the confusion matrix, after EMD decomposition, the classification accuracy of class A and C is higher, and 16% of class B is classified into A. There were serious misclassification in class D, and the accuracy rate was the lowest, 83% of which were classified into class B. After normalization, the classification effect of the

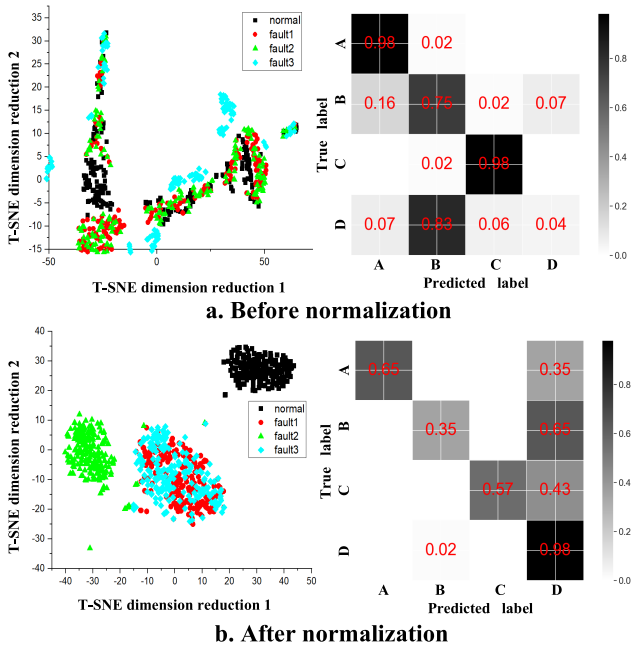

FIGURE 5. T-SNE dimension reduction of multiple entropy features and confusion matrix of classification results by EMD.

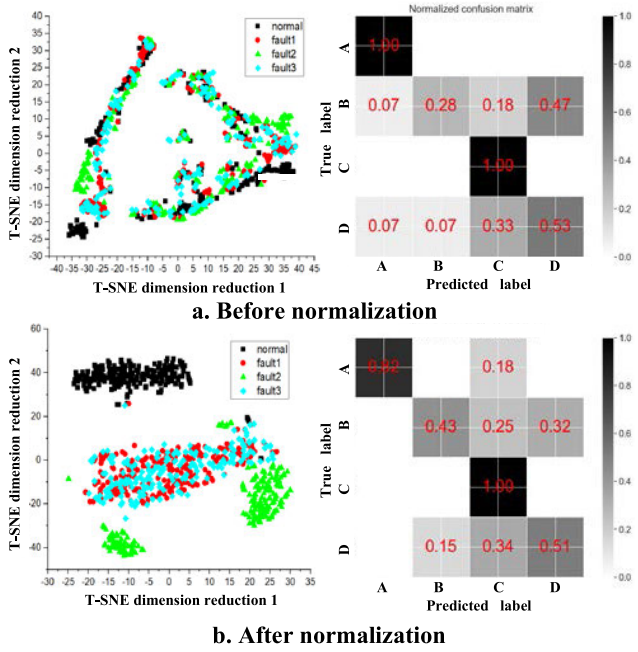

FIGURE 6. T-SNE dimension reduction of multiple entropy features and confusion matrix of classification results by EEMD.

three types of problem signals is not significantly improved, and there is still confusion between normal signals and problem signals. After EEMD decomposition, the classification accuracy of class A and C is still high, which indicates that the collected data itself has large discrimination and low performance requirements for the algorithm. However, there are still many misclassifications between class B and D, but the confusion between normal signals and problem signals has been improved to a certain extent. It can be considered that normalization is helpful for dimensionality reduction, but the improvement of LSSVM classification effect is limited.

Fig. 7, 8 shows the reduced dimension visualization of t-SNE with multiple entropy features after CEEMD CEEMDAN decomposition and the confusion matrix diagram of classification results with unoptimized LSSVM. Compared with figure 5 and figure 6, it can be seen that the clustering effect between different states is significantly improved, especially that it is still difficult to distinguish between normal state and fault 2. After using CEEMDAN to decompose, the clustering effect is obviously better than the other three algorithms. According to the results of confusion matrix, the classification accuracy of class A and C is still high. Using CEEMD to decompose, there are still many misclassifications in class B, of which 28% are classified as A and 66% as D. Using CEEMDAN decomposition, the classification effect of class B and D is improved, and the misclassification is basically the confusion of the two kinds of problems. In general, the feature set constructed by CEEMDAN decomposition and normalization has the best comprehensive performance on the data used in this paper.

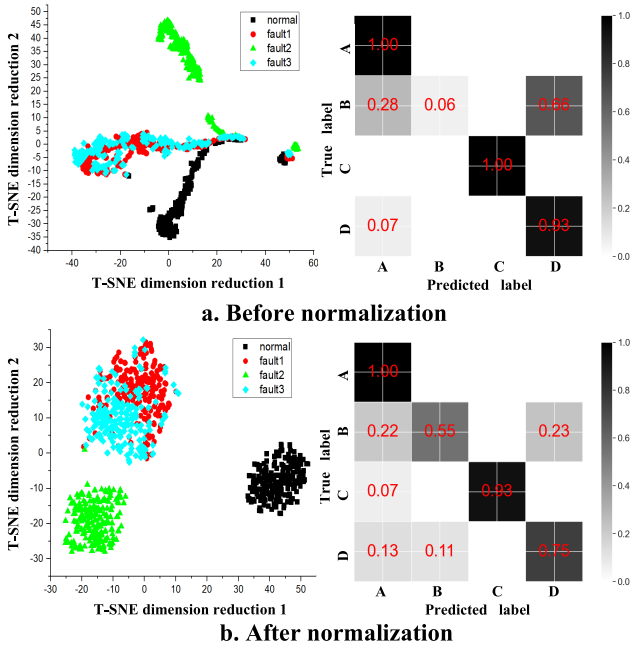

FIGURE 7. T-SNE dimension reduction of multiple entropy features and confusion matrix of classification results by CEEMD.

B. FUSION ENTROPY FEATURE EXTRACTION

In order to evaluate the performance of the entropy features, CEEMDAN is used to decompose and normalize the data. Permutation entropy, energy entropy, and fuzzy entropy are extracted. LSSVM is used for training and testing. The parameters of LSSVM are the same as the previous paper.

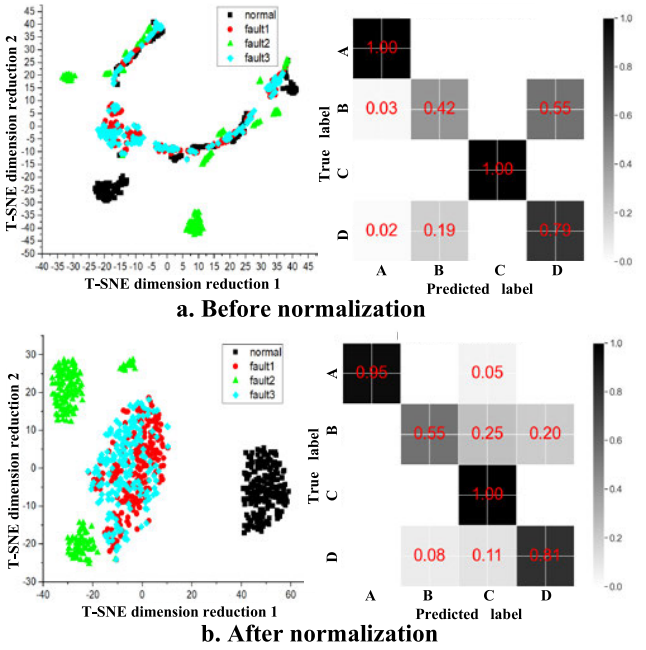

FIGURE 8. T-SNE dimension reduction of multiple entropy features and confusion matrix of classification results by CEEMDAN.

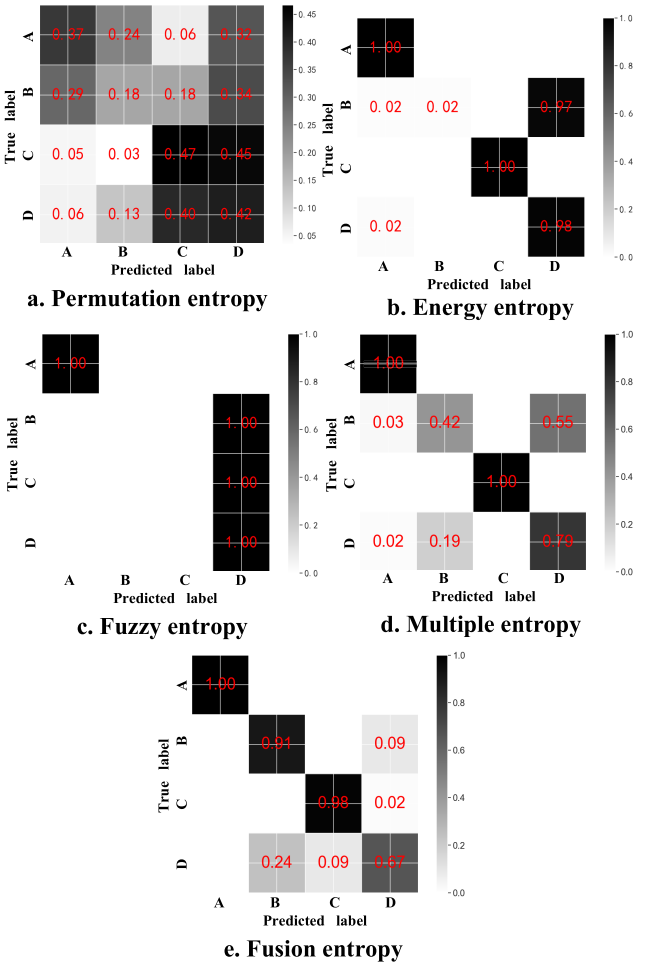

FIGURE 9. Confusion matrix of different entropy classification effect.

As shown in Figure 9, the confusion matrix of the test results of different entropy features is shown.

Permutation entropy is mainly used to evaluate the periodicity and randomness of data. In Figure 9, sub-graph a is the confusion matrix of LSSVM classification results after permutation entropy decomposition. It can be seen that the overall classification effect is poor, but the misclassification situation is not balanced in the four labels. Permutation entropy features of class A and B are closer and easier to be confused, while C and D are more likely to be confused, indicating that the generation of related problems has great influence on the periodicity of signal data. Although permutation entropy cannot accurately distinguish the problem signals, it has a certain value for the signal classification of combine assembly quality problems collected in this paper. Energy entropy can reflect the distribution of signal energy in each component. Sub-graph b in Figure 8 is the LSSVM classification result after energy entropy decomposition, and the overall classification accuracy reaches 75%. It can be seen that class A, C and D have better classification effect, while B has all misclassification, indicating that energy entropy features, as a global feature, has good performance, but it is easy to ignore the information brought by weak changes. Fuzzy entropy mainly reflects the degree of confusion between the front and back parts of the data. Sub-graph c in Figure 8 is the classification result of LSSVM using fuzzy entropy features. It can be seen that the overall classification situation is relatively simple, and the degree of confusion is low. All class A and D are correctly classified, while B and C were wrongly classified as D. It shows that fuzzy entropy futures, can effectively distinguish normal signals from problem signals, but the performance of distinguishing between problems is poor.

In order to improve the performance of features, the above three entropy features are combined to form a new 30 dimensional comprehensive feature set. The three entropy features are fused by KPCA to construct a complementary fusion feature set with the same dimension as a single entropy. After all samples decomposed by CEEMDAN, the multiple entropy extracted from the first 13th IMF respectively, then the fusion feature set obtained by the KPCA. In order to verify the effect of KPCA and ensure the same dimension of feature set before and after decomposition, the principal component score is set to 13. The choice of kernel function and parameter σ of KPCA affect the performance directly. Grid search tool from scikit-learn is used to optimize the KPCA. The results show that when sigmoid kernel function is selected and parameter σ is 0.05, the classification effect is the best. As shown in Figure 9, Sub-graph d is the LSSVM classification effect of feature set composed of multiple entropy, and Sub-graph e is the LSSVM classification result after KPCA fusion optimized by multiple entropy. It can be seen that the

classification performance of a simple feature set with multiple entropy features is better than that of subgraphs a, b and c, but the feature dimension is increased to 39, and the confusion between B and D is still very obvious. The fusion features optimized by KPCA not only reduce the dimension of feature information, but also retain the advantages of the multiple entropy. It has high accuracy in distinguishing class A and class C, especially for class B and class D, the performance has been significantly improved.

C. OPTIMIZED LSSVM

In order to further improve the performance of LSSVM classifier, the genetic algorithm (GA), particle swarm optimization (PSO) and whale optimization algorithm (WOA) are used to optimize LSSVM, then the results are analyzed. In LSSVM, the regularization parameter Gama can affect the model complexity and empirical risk, which is too large to cause over fitting, and too small to cause poor results; the kernel function parameter Sigma determines the linear mapping model, which is directly related to the classification results. Therefore, the Gama and Sigma are selected for optimization. The process of the three optimization can be shown in Figure 10.

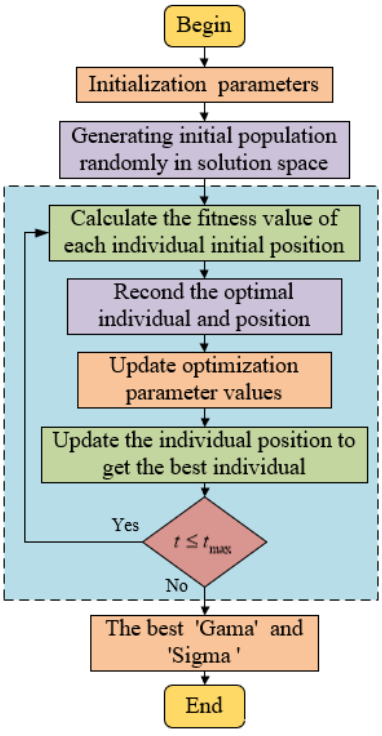

FIGURE 10. Flow chart of optimization algorithm.

The range of Gama and Sigma of LSSVM is set to [0,50]. Initialization the WOA Hyperparameters, set the number of population $n = 100$, the maximum number of iterations $t_{\max} = 20$, logarithmic spiral constant $b = 0.5$, random number $I = 0.8$. The population size and the maximum number of iterations of PSO and GA are set to the same value, the rest

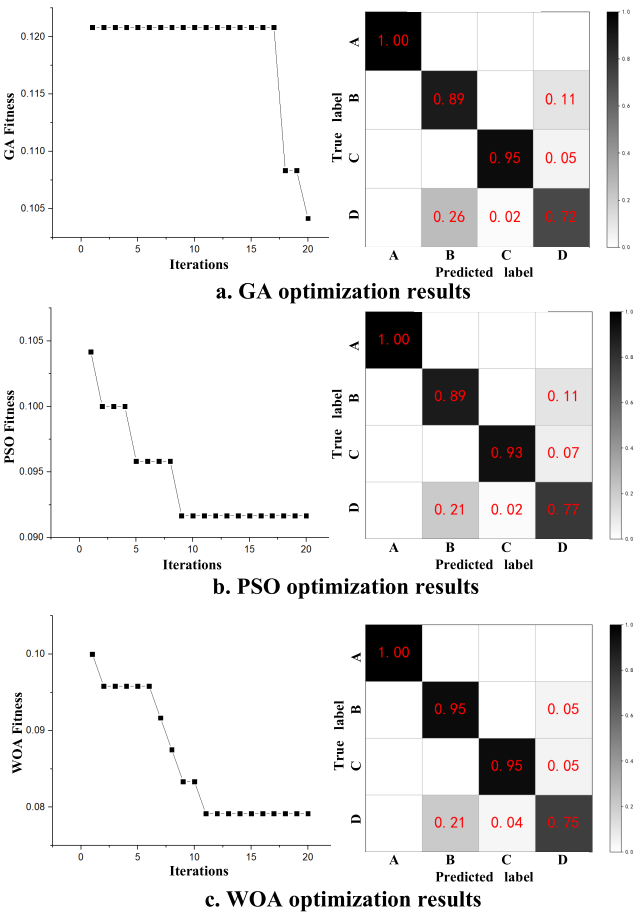

FIGURE 11. LSSVM optimized fitness curve and confusion matrix.

parameters adopt the default. The best classification accuracy of the data set on the least squares support vector machine is taken as the fitness function for optimization. The population is randomly generated in the solution space, and the fitness value of each individual is calculated, and the optimal fitness position is taken as the prey position. Update the parameters and the whale position information according to the rules, get the optimal position and record it. Determine whether the maximum number of iterations is reached. If the conditions are met, output the optimal value and the optimal individual position, otherwise continue to search. After optimization, the WOA optimization parameters are Gama = 5.5, Sigma = 1.9, GA optimization parameters are Gama = 3.2, Sigma = 1.35, and PSO optimization parameters are Gama = 4.78, Sigma = 1.51. The optimized parameters are brought into LSSVM model, and the results as follows after training and testing.

Table 2 shows the classification results of LSSVM optimized by different data sets. It can be seen that the overall classification accuracy of single entropy is poor. After integrating multiple entropy, the accuracy is improved due to the improvement of data dimension. After using the fusion entropy feature, the overall classification effect is better than others, especially after WOA optimization, the accuracy reaches the highest.

TABLE 2. Comparison of classification accuracy of different feature extraction methods.

Different methods	Permutation Entropy	Fuzzy Entropy	Energy Entropy	Multiple Entropy	Fusion Entropy
				Classification Accuracy（%）	
LSSVM	71.5	70.5	62.5	82.5	89
PSO-SVM	\	\	\	85.83	90.5
WOA-LSSVM	\	\	\	92.52	94.25

Figure 12 shows the fitness curve and classification test confusion matrix of LSSVM model optimized by GA, PSO and WOA. In the LSSVM model test results after WOA optimization, the classification accuracy of class A, B and C is more than 95%, and the classification accuracy of class B is 4% higher than that of unoptimized, and 6% higher than that of GA and PSO optimization. The classification accuracy of class D is 8% higher than that of unoptimized and 3% higher than that of GA optimization. In general, the final classification accuracy of WOA is 92.1%, which is better than the GA 89.6%, PSO 90.5%, and unoptimized 87.9%. It can be seen that the fault diagnosis model of WOA optimized LSSVM based on CEEMDAN decomposition and multi-entropy KPCA fusion features proposed in this paper can accurately identify the faults of combine in different states, and can be applied to the assembly quality detection of combine.

It can be seen from the fitness curve in Figure 11 that the WOA optimization iterative process is smoother than that of GA and PSO, which indicates that the WOA search process has strong target pertinence, large domain search range and better optimization effect. As shown in Table 3, for the data sets and optimization problems in this paper, the optimization time of WOA and GA is 206 seconds and 200 seconds respectively, which is much shorter than that of PSO's 464 seconds, reflecting the characteristics of WOA, such as fast convergence speed, simple execution process, less solving parameters and low computational complexity. In general, WOA, as a new heuristic optimization algorithm, has better comprehensive performance than GA and PSO in the case of the same number of population and iterations. Especially for the data set and LSSVM in this paper, the optimization effect and performance is the best.

TABLE 3. Running time of the optimization.

Different methods	GA	PSO	WOA
Optimization running time	200 s	464 s	206 s

V. CONCLUSION

(1) Analysis the performance of adaptive decomposition algorithm in combine assembly quality detection. According to the strong noise characteristics of combine vibration signal, CEEMDAN can extract useful assembly quality problem features more accurately.

(2) Based on the decomposition of CEEMDAN, the performance of Permutation entropy, Fuzzy entropy and Energy entropy in combine assembly quality detection is analyzed. By optimizing KPCA, a variety of entropy fusion feature sets are constructed, and the results show that this method has the best performance in the detection of combine assembly quality.

(3) By optimizing LSSVM, the accuracy of combine assembly quality detection method is further improved, especially the classification accuracy after using WOA optimization and the multiple entropy fusion feature set proposed in this paper to train LSSVM, which has a certain practical significance for the follow-up research.

REFERENCES

[1] Q. W. Chen, Z. D. Han, J. W. Cui, G. X. Wang, X. D. Qiao, Z. R. Zhang, and B. X. Gan, "Development status and trend current situation of self-propelled combine harvester," *J. Agricult. Sci. Technol.*, vol. 17, no. 1, pp. 109–114, 2015, doi: 10.13304/j.nykjdb.2015.042.

[2] Z. Gao, L. Xu, Y. Li, Y. Wang, and P. Sun, "Vibration measure and analysis of crawler-type rice and wheat combine harvester in field harvesting condition," *Trans. Chin. Soc. Agricult. Eng.*, vol. 33, no. 20, pp. 48–55, 2017, doi: 10.11975/j.issn.1002-6819.2017.20.006.

[3] S. Chen, Y. Zhou, Z. Tang, and S. Lu, "Modal vibration response of rice combine harvester frame under multi-source excitation," *Biosyst. Eng.*, vol. 194, pp. 177–195, Jun. 2020, doi: 10.1016/j.biosystemseng.2020.04.002.

[4] L. Yaoming, P. Jing, X. Lizhang, T. Zhong, and Z. Yuepeng, "Manufacturing defect location of cleaning screen of grain combine harvester based on vibration excitation tracing," *Trans. Chin. Soc. Agricult. Eng.*, vol. 35, no. 5, pp. 10–17, 2019, doi: 10.11975/j.issn.1002-6819.2019.05.002.

[5] C. Shuren, L. Qiang, and Q. Huazheng, "Header vibration analysis of grain combine harvester based on LabVIEW," *Trans. Chin. Soc. Agricult. Mach.*, vol. 42, no. S1, pp. 86–89, 2011, doi: 10.3969/j.issn.1000-1298.2011.S0.020.

[6] Y. Zhang, D. Wang, D. Chen, S. Wang, and H. Fu, "Online method for large-scale harvester engine punch combination position accuracy measurement," *Trans. Chin. Soc. Agricult. Mach.*, vol. 48, no. S1, pp. 71–78, 2017, doi: 10.6041/j.issn.1000-1298.2017.S0.012.

[7] W. Zhong, L. Peng, Y.-G. Zhou, J. Xu, and F.-Y. Cong, "Slagging diagnosis of boiler based on wavelet packet analysis and support vector machine," *J. Zhejiang Univ. Eng. Sci.*, vol. 50, no. 8, pp. 1499–1506, 2016, doi: 10.3785/j.issn.1008-973X.2016.08.011.

[8] T. T. Chowdhury, S. A. Fattah, and C. Shahnaz, "Seizure activity classification based on bimodal Gaussian modeling of the gamma and theta band IMFs of EEG signals," *Biomed. Signal Process. Control*, vol. 64, Feb. 2021, Art no. 102273, doi: 10.1016/j.bspc.2020.102273.

[9] Y. Zhang, B. Yan, and M. Aasma, "A novel deep learning framework: Prediction and analysis of financial time series using CEEMD and LSTM," *Expert Syst. Appl.*, vol. 159, Nov. 2020, Art. no. 113609, doi: 10.1016/j.eswa.2020.113609.

[10] M. K. Babouri, N. Ouelaa, T. Kebabsa, and A. Djebala, "Diagnosis of mechanical defects using a hybrid method based on complete ensemble empirical mode decomposition with adaptive noise (CEEMDAN) and optimized wavelet multi-resolution analysis (OWMRA): Experimental study," *Int. J. Adv. Manuf. Technol.*, vol. 112, nos. 9–10, pp. 2657–2681, Feb. 2021, doi: 10.1007/s00170-020-06496-z.

[11] N. S. Haider, "Respiratory sound denoising using empirical mode decomposition, hurst analysis and spectral subtraction," *Biomed. Signal Process. Control*, vol. 64, Feb. 2021, Art. no. 102313, doi: 10.1016/j.bspc.2020.102313.

[12] Y. Zhan, L. Cheng, and W. T. , "Fault diagnosis performance optimization method based on decorrelation multi-frequency EMD," *J. Vib. Shock*, vol. 39, no. 1, pp. 115–122 and 149, 2020, doi: 10.13465/j.cnki.jvs.2020.01.017.

[13] Z. Wu and N. E. Huang, "Ensemble empirical mode decomposition: A noise-assisted data analysis method," *Adv. Adapt. Data Anal.*, vol. 1, no. 1, pp. 1–41, Jan. 2009, doi: 10.1142/S1793536909000047.

[14] J.-R. Yeh, J.-S. Shieh, and N. E. Huang, "Complementary ensemble empirical mode decomposition: A novel noise enhanced data analysis method," *Adv. Adapt. Data Anal.*, vol. 2, no. 2, pp. 135–156, Apr. 2010, doi: 10.1142/S1793536910000422.

[15] J. Ma, L. Zhan, C. Li, and Z. Li, "An improved intrinsic time-scale decomposition method based on adaptive noise and its application in bearing fault feature extraction," *Meas. Sci. Technol.*, vol. 32, no. 2, Feb. 2021, Art. no. 025103, doi: 10.1088/1361-6501/abbc48.

[16] J. R. Zhang, H. Tang, W. Tao, J. Ma, Q. Tan, D. Xia, X. Liu, and Y. Zhang, "A hybrid landslide displacement prediction method based on CEEMD and DTW-ACO-SVR—Cases studied in the three gorges reservoir area," (in English), *Sensors*, vol. 20, no. 15, p. 4287, Aug. 2020, doi: 10.3390/s20154287.

[17] D. X. Niu, K. K. Wang, L. J. Sun, J. Wu, and X. M. Xu, "Short-term photovoltaic power generation forecasting based on random forest feature selection and CEEMD: A case study," (in English), *Appl. Soft. Comput.*, vol. 93, Aug. 2020, Art. no. 106389, doi: 10.1016/j.asoc.2020.106389.

[18] L. Yao and Z. Pan, "A new method based CEEMDAN for removal of baseline wander and powerline interference in ECG signals," *Optik*, vol. 223, Dec. 2020, Art. no. 165566, doi: 10.1016/j.ijleo.2020.165566.

[19] X. Cheng, J. Mao, J. Li, H. Zhao, C. Zhou, X. Gong, and Z. Rao, "An EEMD-SVD-LWT algorithm for denoising a Lidar signal," *Measurement*, vol. 168, Jan. 2021, Art. no. 108405, doi: 10.1016/j.measurement.2020.108405.

[20] J. Xiang, Y. Lei, Y. Wang, Y. He, C. Zheng, and H. Gao, "Structural dynamical monitoring and fault diagnosis," *Shock Vibrat.*, vol. 2015, no. 193831, pp. 1–3, 2015, doi: 10.1155/2015/193831.

[21] R. J. Romero-Troncoso, R. Saucedo-Gallaga, E. Cabal-Yepez, A. Garcia-Perez, R. A. Osornio-Rios, R. Alvarez-Salas, H. Miranda-Vidales, and N. Huber, "FPGA-based online detection of multiple combined faults in induction motors through information entropy and fuzzy inference," *IEEE Trans. Ind. Electron.*, vol. 58, no. 11, pp. 5263–5270, Nov. 2011, doi: 10.1109/tie.2011.2123858.

[22] L. Zhang, G. Xiong, H. Liu, H. Zou, and W. Guo, "Bearing fault diagnosis using multi-scale entropy and adaptive neuro-fuzzy inference," *Expert Syst. Appl.*, vol. 37, no. 8, pp. 6077–6085, Aug. 2010, doi: 10.1016/j.eswa.2010.02.118.

[23] C.-W. Fei, G.-C. Bai, W.-Z. Tang, and S. Ma, "Quantitative diagnosis of rotor vibration fault using process power spectrum entropy and support vector machine method," *Shock Vibrat.*, vol. 2014, pp. 1–9, Mar. 2014, doi: 10.1155/2014/957531.

[24] Y.-T. Ai, J.-Y. Guan, C.-W. Fei, J. Tian, and F.-L. Zhang, "Fusion information entropy method of rolling bearing fault diagnosis based on n-dimensional characteristic parameter distance," *Mech. Syst. Signal Process.*, vol. 88, pp. 123–136, May 2017, doi: 10.1016/j.ymssp.2016.11.019.

[25] J. Tian, Y. Ai, C. Fei, M. Zhao, F. Zhang, and Z. Wang, "Fault diagnosis of intershaft bearings using fusion information exergy distance method," *Shock Vibrat.*, vol. 2018, pp. 1–8, Aug. 2018, doi: 10.1155/2018/7546128.

[26] H. M. Li, J. Y. Huang, X. W. Yang, J. Luo, L. D. Zhang, and Y. Pang, "Fault diagnosis for rotating machinery using multiscale permutation entropy and convolutional neural networks," (in English), *Entropy*, vol. 22, no. 8, p. 851, Aug. 2020, doi: 10.3390/e22080851.

[27] B. Yin, X. Lin, W. Tang, and Z. Jin, "Thruster fault identification for autonomous underwater vehicle based on time-domain energy and time-frequency entropy of fusion signal," in *Proc. 12th Int. Conf. Intell. Robot. Appl. (ICIRA)*, in Lecture Notes in Artificial Intelligence, vol. 11742, H. Yu, J. Liu, L. Liu, Z. Ju, Y. Liu, and D. Zhou, Eds. Springer-Verlag, Aug. 2019, pp. 264–275.

[28] L. Min, H. Jie, and X. Sun, "A hydraulic fault diagnosis method based on IMF entropy feature fusion," *J. Phys., Conf. Ser.*, vol. 1187, no. 3, Apr. 2019, Art. no. 032041.

[29] S. Gao, T. Li, and Y. Zhang, "Rolling bearing fault diagnosis of PSO–LSSVM based on CEEMD entropy fusion," *Trans. Can. Soc. Mech. Eng.*, vol. 44, no. 3, pp. 405–418, Sep. 2020, doi: 10.1139/tcsme-2019-0114.

[30] Y. Liu, X. Zhang, and Y. Yu, "A fast entropy assisted complete ensemble empirical mode decomposition algorithm," in *Proc. 2nd Int. Conf. Syst. Informat. (ICSAI)*, Shanghai, China, Nov. 2014, pp. 697–701, doi: 10.1109/ICSAI.2014.7009375.

[31] Q. Zhang, Y. Li, G. Zhao, P. Man, Y. Lin, and M. Wang, "A novel algorithm for breast mass classification in digital mammography based on feature fusion," *J. Healthcare Eng.*, vol. 2020, pp. 1–11, Dec. 2020, doi: 10.1155/2020/8860011.

[32] M. Li, R. Wang, and D. Xu, "An improved composite multiscale fuzzy entropy for feature extraction of MI-EEG," *Entropy*, vol. 22, no. 12, p. 1356, Nov. 2020, doi: 10.3390/e22121356.

[33] T.-K. Lin and Y.-H. Chien, "Performance evaluation of an entropy-based structural health monitoring system utilizing composite multiscale cross-sample entropy," *Entropy*, vol. 21, no. 1, p. 41, Jan. 2019, doi: 10.3390/e21010041.

[34] J. Zhao and Y. Liu, "Approximate entropy based on Hilbert transform and its application in bearing fault diagnosis," in *Proc. Int. Conf. Sens., Diagnostics, Prognostics, Control (SDPC)*, Aug. 2018, pp. 41–44.

[35] Y. Li, X. Wang, S. Si, and S. Huang, "Entropy based fault classification using the case western reserve university data: A benchmark study," *IEEE Trans. Rel.*, vol. 69, no. 2, pp. 754–767, Jun. 2020, doi: 10.1109/tr.2019.2896240.

[36] Y. Li, Y. Yang, X. Wang, B. Liu, and X. Liang, "Early fault diagnosis of rolling bearings based on hierarchical symbol dynamic entropy and binary tree support vector machine," *J. Sound Vibrat.*, vol. 428, pp. 72–86, Aug. 2018, doi: 10.1016/j.jsv.2018.04.036.

[37] C.-P. Wei, P. Wang, and Y.-Z. Zhang, "Entropy, similarity measure of interval-valued intuitionistic fuzzy sets and their applications," *Inf. Sci.*, vol. 181, no. 19, pp. 4273–4286, Oct. 2011, doi: 10.1016/j.ins.2011.06.001.

[38] J. Zheng, H. Pan, S. Yang, and J. Cheng, "Generalized composite multiscale permutation entropy and Laplacian score based rolling bearing fault diagnosis," *Mech. Syst. Signal Process.*, vol. 99, pp. 229–243, Jan. 2018, doi: 10.1016/j.ymssp.2017.06.011.

[39] X. Zhang, Y. Liang, J. Zhou, and Y. Zang, "A novel bearing fault diagnosis model integrated permutation entropy, ensemble empirical mode decomposition and optimized SVM," *Measurement*, vol. 69, pp. 164–179, Jun. 2015, doi: 10.1016/j.measurement.2015.03.017.

SIXIA ZHAO (Member, IEEE) received the B.S. degree in mechanical engineering and automation from Henan Polytechnic University, Jiaozuo, China, in 2013, and the M.S. degree in mechanical engineering from the Henan University of Science and Technology, Luoyang, China, in 2018, where he is currently pursuing the Ph.D. degree. His research interests include fault diagnosis of agricultural machinery and new transmission system of agricultural vehicles.

LIYOU XU (Member, IEEE) received the B.S. degree in mechanical manufacturing technology and equipment from the Jiaozuo Institute of Technology, Jiaozuo, China, in 1998, the M.S. degree in vehicle engineering from the Luoyang Institute of Technology, Luoyang, China, in 2018, and the Ph.D. degree in vehicle engineering from the Xi'an University of Technology, Xi'an, in 2007. Since 2013, he has been a Professor with the College of Vehicle and Traffic Engineering, Henan University of Science and Technology, Luoyang, China. His research interests include new transmission theory and control technology, vehicle performance analysis method and simulation technology, and low-speed electric vehicle transmission technology.

JIAMING ZHANG received the bachelor's degree in mechanical design, manufacturing, and automation from the Luoyang Institute of technology. He is currently pursuing the master's degree in vehicle engineering with the Henan University of science and technology, Luoyang, China. His research interest includes fault diagnosis of combine.

SHUAI ZHANG (Member, IEEE) received the B.S. and M.S. degrees in vehicle engineering from the Henan University of Science and Technology, Luoyang, China, in 2011 and 2014, respectively, and the Ph.D. degree in vehicle engineering from Jilin University, Jilin, China, in 2018. Since 2018, he has been a Lecturer with the College of Vehicle and Traffic Engineering, Henan University of Science and Technology. His research interests include research and innovation of automobile structure design theory, and key technology.

XIAOLIANG CHEN (Member, IEEE) received the B.S. degree in agricultural mechanization and automation from the Henan University of Science and Technology, Luoyang, China, in 2009, and the M.S. degree in mechanical design and theory from Zhejiang Sci-Tech University, Hangzhou, China, in 2013. He is currently pursuing the Ph.D. degree with the Henan University of Science and Technology. His research interests include fault diagnosis of agricultural machinery and NVH.

JUN WEI (Member, IEEE) received the B.S. degree from the College of Agricultural Equipment Engineering, Henan University of Science and Technology, Luoyang, China, where he is currently pursuing the master's degree in vehicle engineering. His research interest includes fault diagnosis of combine harvester.